sensors

Near infrared spectroscopy as a rapid screening method for the determination of total anthocyanin content in sambucus fructus

Supplementary Materials

Stefan Stuppner[1,2], Sophia Mayr[1], Anel Beganovic[1], Krzysztof Beć[1], Justyna Grabska[1], Urban Aufschnaiter[1], Magdalena Groeneveld[1], Matthias Rainer[1], Thomas Jakschitz[2], Günther K. Bonn[1,2] and Christian W. Huck[1,*]

[1] Institute of Analytical Chemistry and Radiochemistry, Leopold-Franzens University Innsbruck, Innrain 80-82, 6020 Innsbruck, Austria
[2] ADSI-Austrian Drug Screening Institute GmbH, Innrain 66A, 6020 Innsbruck, Austria
* Correspondence: Christian.W.Huck@uibk.ac.at; Tel.: +43 512 507 57304

Table S1. Latitude and Longitude of the Elderberry collection.

Sample description	degree of longitude / °O	degree of latitude / °E
S1	11°22'30,35028"	47°15'48,42936"
S3	11°21'2984544"	47°15'20,46024"
S6	11°22'33,681"	47°15'26,35812"
S7	11°21'57,66696"	47°15'38,7522"
S9	11°22'456456"	47°15'30,924"
S10	11°22'12,5202"	47°16'24,58056"
S11	11°22"12,85788"	47°16'27,5994"
S12	11°22'12,1188"	47°16'21,8442"
S13	11°22'12522"	47°16'23,52216"
S14	11°21'57,21372"	47°16'15,58992"
S15	11°21'32,110548"	47°16'21,20982"
S16	11°23'51,4186"	47°16'16,05612"
S17	11°25'10,6356"	47°15'40,2264"
S18	11°21'26,369"	47°15'20,47"
S19	11°22'33,344"	47°15'26,654"
S20	11°21'58,946"	47°15'13,727"
S21	11°21'40,273"	47°15'17,05"
S22	11°15'0,651"	47°13'47,658"
S23	11°19'41,30124"	47°14'50,91936"
S24	11°18'57,42804"	47°14'49,97796"
R1	10°92’35,651‘‘	47°22’27,558‘‘
R2	10°92’35,651‘‘	47°22’27,558‘‘
R3	10°92’35,16‘‘	47°22’33,04‘‘
R4	10°92’35,16‘‘	47°22’33,04‘‘
R5	10°92’29,036‘‘	47°22’32,809‘‘
R6	10°92’29,036	47°22’32,809‘‘
R7	10°92’29,036‘‘	47°22’32,809‘‘

Table S2. Validation of pH differential method.

	Day 1	**Day 2**	**Day 3**
1	2638.59	2266.87	2008.88
2	2696.87	2275.22	2054.8
3	2661.8	2274.39	1985.5
4	2621.72	2213.44	2020.57
5	2600.02	2244.33	2064.82
6	2575.8	2342.02	2160.84
7	2622.56	2311.96	2090.7
8	2655.96	2349.53	2050.62
9	2598.35	2347.86	2097.38
10	2712.73	2299.44	2176.7
Mean	2638.34	2292.51	2071.08
Standarddeviation	44	46	62
RSD	2%	2%	3%

Table S3. Band assigments for cyanidin-3-O-sambubioside (compare with Fig. S10).

Wavenumber [cm^{-1}]	**Assignment** [a)]
6961.885	2νOH
6846.014	2νOH
6861.453	2νOH
6785.449	2νOH
6757.406	2νOH
6717.978	2νOH
6558.512	2νOH
6505.660	2νOH
6286.199	2νOH
6270.684	2νOH
6195.627	νCH + νOH
6005.357	νCH + νOH
5904.773	νCH + νOH
5275.323	2νCH
5096.103	(νCOH, ν_{ring}) + νOH
5083.253	(νCOH, ν_{ring}) + νOH
5058.789	(νCOH, ν_{ring}) + νOH
5010.365	(νCOH, ν_{ring}) + νOH
4694.44	(νCOH, ν_{ring}) + νOH
4753.352	(νCOH, ν_{ring}) + νOH
4813.062	νCOH + νOH
4892.365	(νCOH, ν_{ring}) + νOH
4553.383	(νCOH, ν_{ring}) + νOH
4508.411	$\nu_{wagg}CH_2$ + νOH
4471.086	ν_{ring} + νOH
4293.658	ν_{ring} +νCH

4165.276	ν$_{oop}$COH + νOH
4064.083	νCOH + νCH
4039.047	ν$_{ring}$ + νCH

[a] Notation used: "2" denotes first overtones; "+" sign denotes combination transitions; ν - stretching mode; δ - deformation mode; as – antisymmetric; s – symmetric (mode).

Table S4. Band assigments for cyanidin-3-Osambubioside-5-glucoside (compare with Fig. S11).

Wavenumber [cm^{-1}]	**Assignment** [a]
6885	2νOH
6860	2νOH
6795	2νOH
6780	2νOH
6680	2νOH
6645	2νOH
6609	2νOH
6568	2νOH
6318	2νOH
6227	νCH +νOH
6166	νCH +νOH
6114	⊚νCH,ν$_{s}$CH$_2$]+νOH
6063	⊚νCH,ν$_{as}$CH$_2$]+νOH
6024	⊚νCH,ν$_{as}$CH$_2$]+νOH
5933	⊚νCH,ν$_{as}$CH$_2$]+νOH
5905	⊚νCH,ν$_{as}$CH$_2$]+νOH
5411	2νCH
5325	⊚νCH,ν$_{s}$CH$_2$]+⊚⊚νCH,ν$_{s}$CH$_2$]
5278	⊚νCH,ν$_{as}$CH$_2$]+ν$_{s}$CH$_2$
5235	2νCH, 2ν$_{s}$CH$_2$
5105	⊚⊚ring, ⊚COH]+νOH
5082	⊚⊚ring, ⊚COH]+νOH
5041	νOH +νOH
5025	⊚ring +νOH
4963	⊚⊚ring, ⊚COH]+νOH
4906	⊚⊚ring, ⊚COH]+νOH
4881	⊚COH +νOH
4868	⊚COH +νOH
4831	⊚COH +νOH
4809	⊚COH +νOH
4779	⊚⊚ring, ⊚COH]+νOH
4756	⊚COH⊚⊚νOH
4731	⊚⊚ring, ⊚COH]⊚νOH
4698	⊚⊚ring, ⊚COH]⊚νOH
4624	2νCH, 2ν$_{as}$CH$_2$
4530	⊚⊚COH, ⊚$_{twist}$CH$_2$]⊚⊚νOH
4480	⊚⊚ring,⊚⊚$_{twist}$CH$_2$]⊚νOH
4451	⊚⊚ring,⊚⊚COH,⊚⊚$_{twist}$CH$_2$]⊚νOH
4410	⊚⊚ring,⊚⊚COH,⊚⊚$_{twist}$CH$_2$]⊚νOH
4315	⊚⊚ring, ⊚COH]⊚νCH

4270	⊚⊚ring, ⊚COH]⊚⌁CH
4227	⊚⊚ring, ⊚COH]⊚⌁CH
4178	⊚⊚ring, ⊚COH]⊚⌁CH
4089	⊚⊚ring, ⊚COH]⊚⌁CH
4068	⊚⊚ring, ⊚COH]⊚⌁CH

[(a)] Notation used: "2" denotes first overtones; "+" sign denotes combination transitions; ν - stretching mode; δ - deformation mode; as – antisymmetric; s – symmetric (mode).

Figures

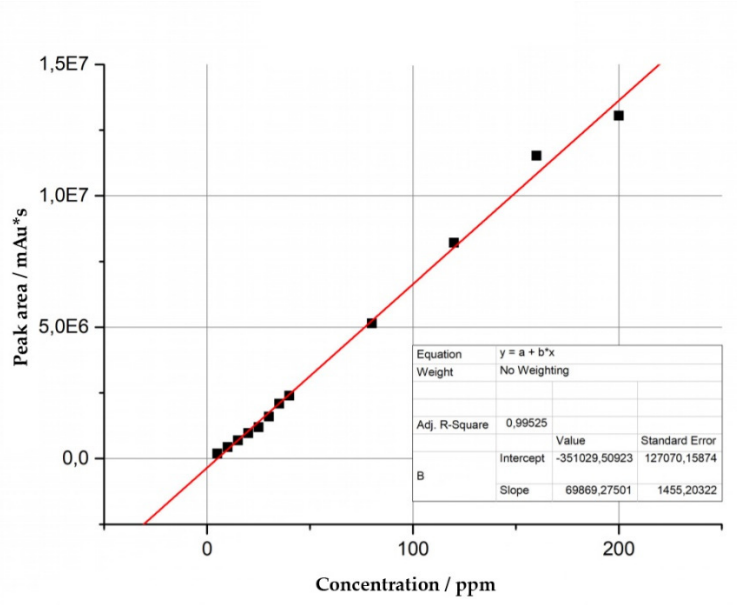

Figure S1. Calibration curve for the reference analysis (UHPLC-MWD-UHR-TOF-MS) of cyanidin-3-O-glucoside.

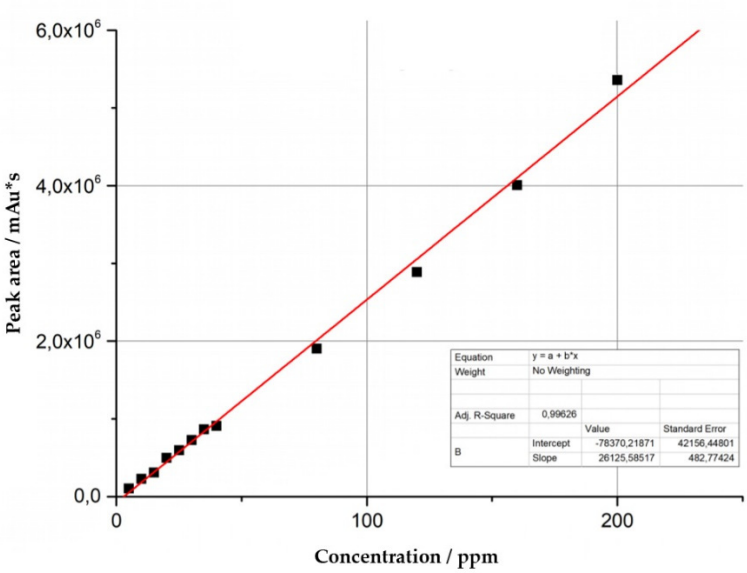

Figure S2. Calibration curve for the reference analysis (UHPLC-MWD-UHR-TOF-MS) of cyanidin-3-O-sambubioside.

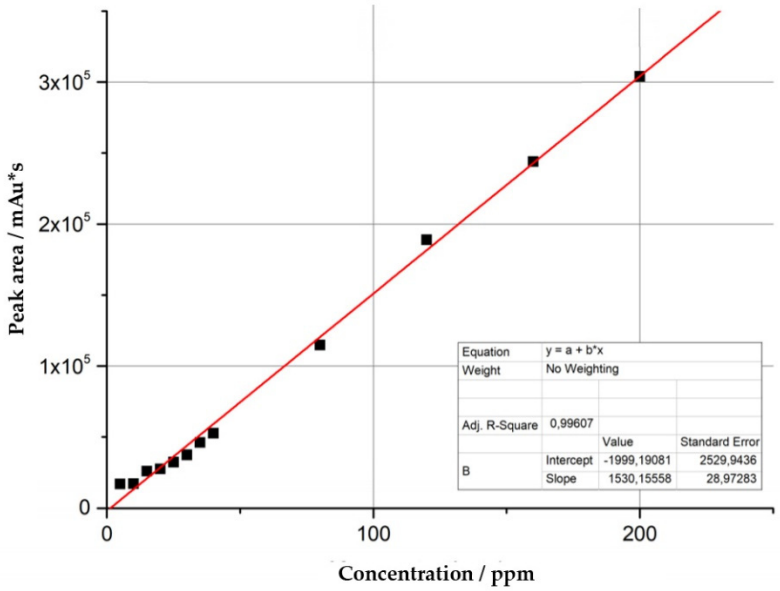

Figure S3. Calibration curve for the reference analysis (UHPLC-MWD-UHR-TOF-MS) of cyanidin-3-Osambubioside-5-glucoside.

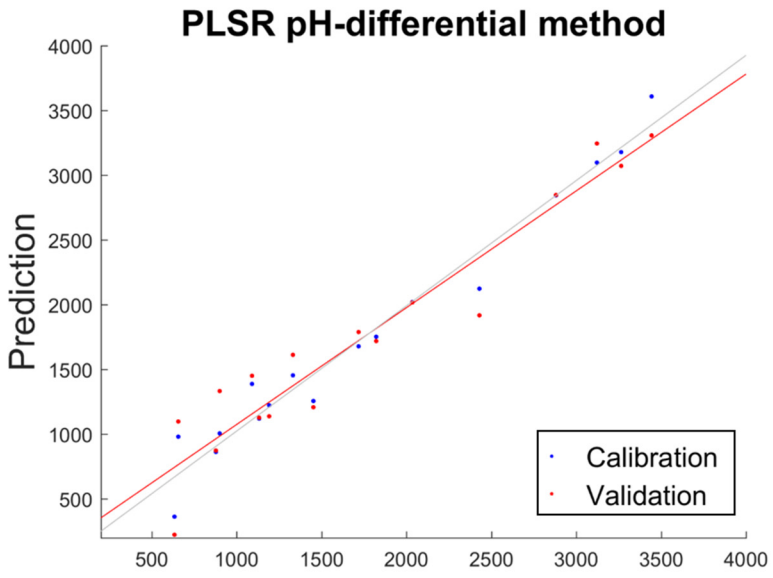

Figure S4. Prediction vs reference plot of NIR data with pH-differential reference method.

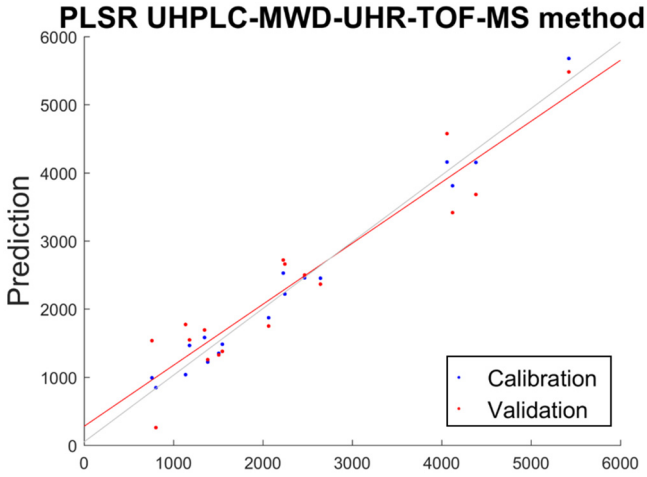

Figure S5. Prediction vs reference plot of NIR data with UHPLC-MWD-UHR-TOF-MS reference method.

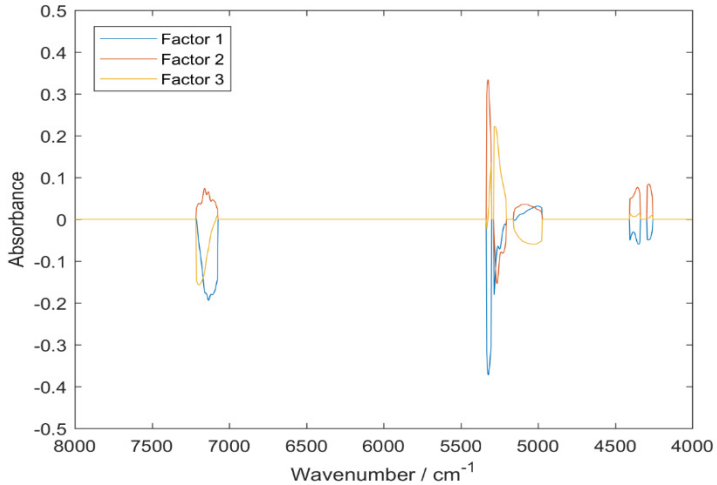

Figure S6. The loadings of the PLSR model correlating NIR spectra of sambucus fructus with pH-differential reference values for TAC content.

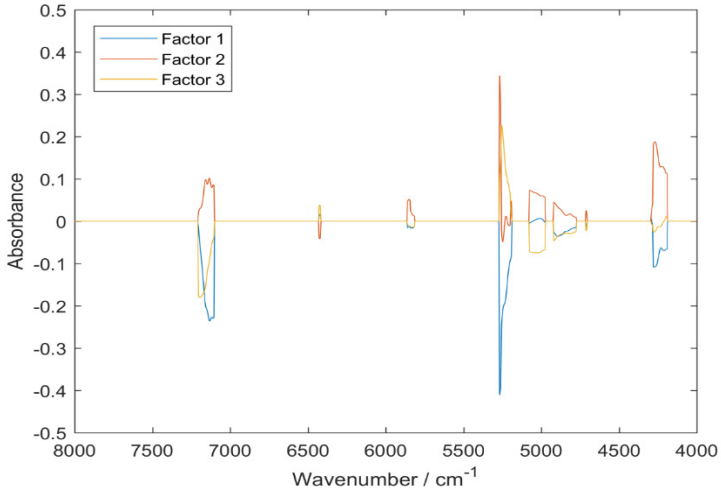

Figure S7. The loadings of the PLSR model correlating NIR spectra of sambucus fructus with UHPLC-MWD-UHR-TOF-MS reference values for TAC content.

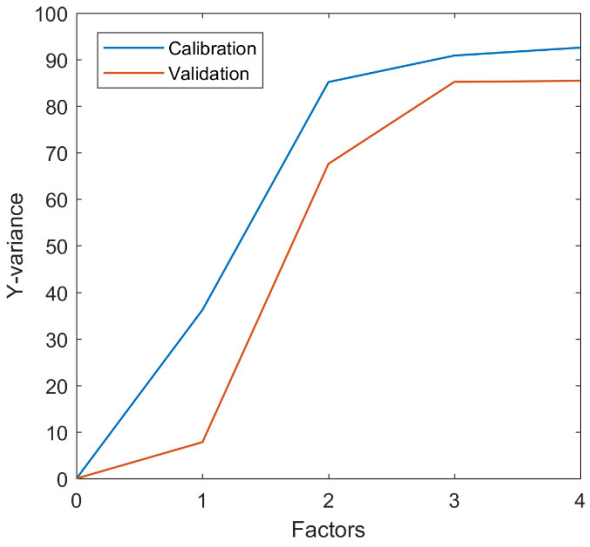

Figure S8. Cumulative explained variance plot of the PLSR model correlating NIR spectra of sambucus fructus with pH-differential reference values for TAC content.

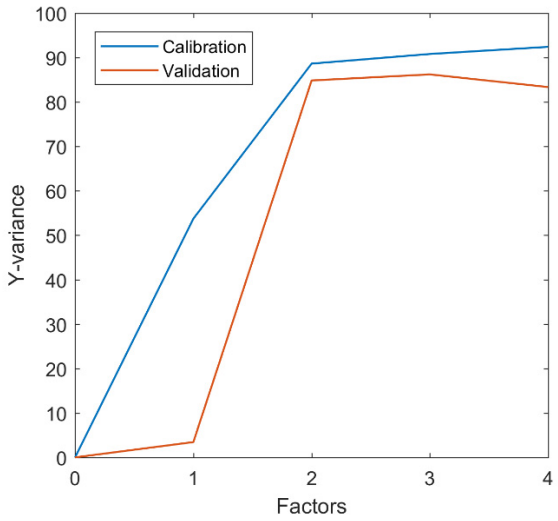

Figure S9. Cumulative explained variance plot of the PLSR model correlating NIR spectra of sambucus fructus with UHPLC-MWD-UHR-TOF-MS reference values for TAC content.

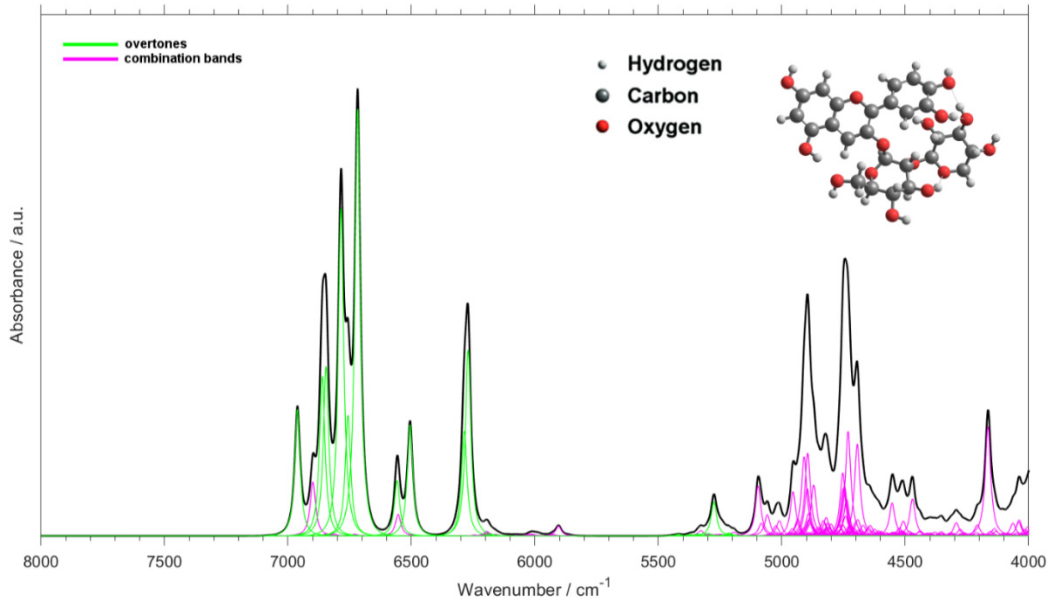

Figure S10. NIR spectrum of cyanidin-3-O-sambubioside simulated with use of quantum chemical calculations. Individual contributing overtone and combination bands are presented.

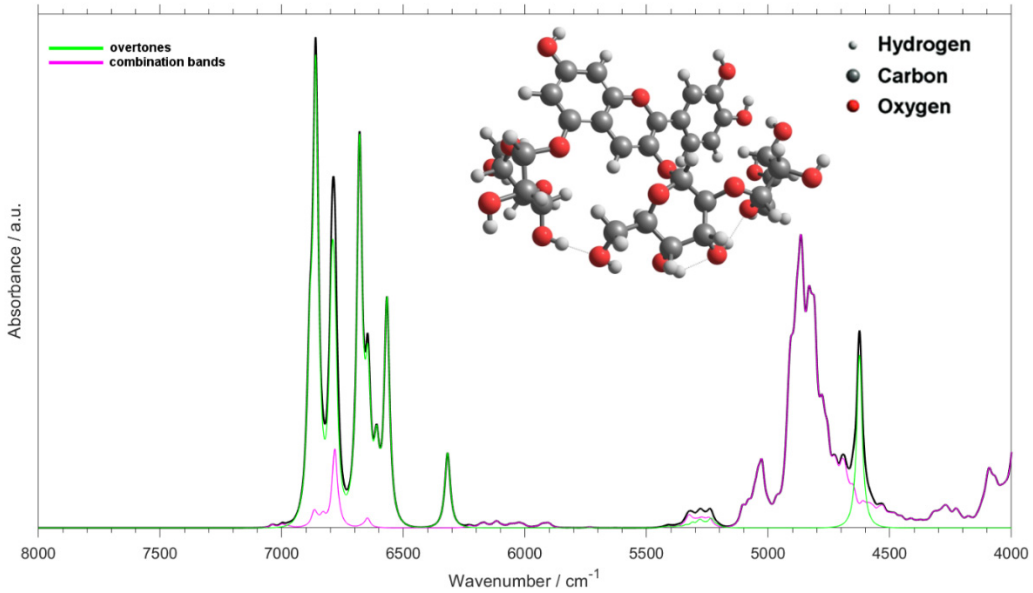

Figure S11. NIR spectrum of cyanidin-3-O-sambubioside-5-O-glucoside simulated with use of quantum chemical calculations. Summed contribution from either overtone or combination bands are presented.

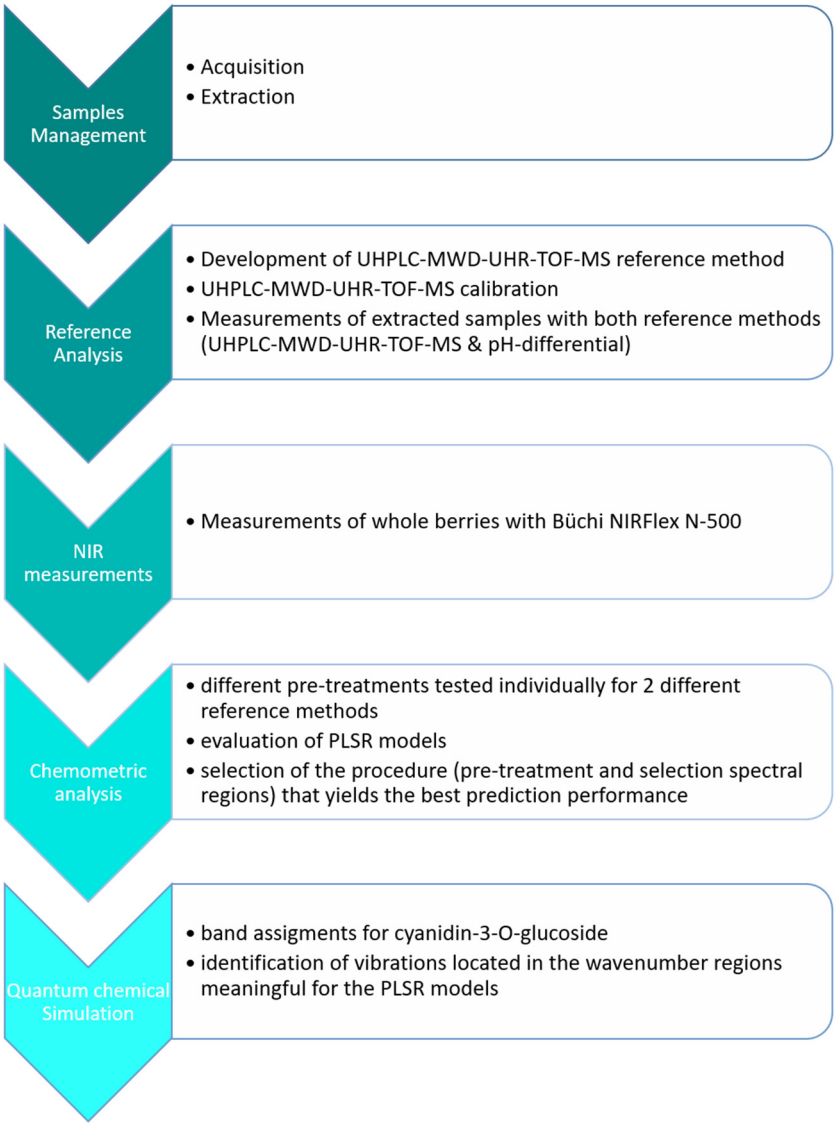

Figure S12. Workflow of the research.